Geological Society of America
Special Paper 419
2007

Finding of high-grade tectonic blocks from the New Idria serpentinite body, Diablo Range, California: Petrologic constraints on the tectonic evolution of an active serpentinite diapir

Tatsuki Tsujimori†
Juhn G. Liou
Robert G. Coleman
Department of Geological and Environmental Sciences, Stanford University, Stanford, California 94305-2115, USA

ABSTRACT

Three high-grade tectonic blocks, including jadeite-bearing retrograded eclogite, pumpellyite-rich retrograded eclogite, and clinopyroxene-bearing garnet-amphibolite, are newly described in the jadeitite-bearing New Idria serpentinite body. Petrologic analyses reveal two contrasting peak metamorphic stages—eclogite-facies metamorphism (M_1^E) characterized by garnet + omphacite (~48 mol% jadeite) + rutile ± epidote + quartz, and amphibolite-facies metamorphism (M_1^A) characterized by garnet + hornblende + augite (~14 mol% jadeite) + rutile + quartz. Both peak metamorphic events are overprinted by very low-*T* blueschist-facies minerals (M_2), which include glaucophane, lawsonite, pumpellyite, jadeitite (up to 94 mol% jadeite), chlorite, and titanite. Garnet-clinopyroxene geothermometry yields T = ~580–620 °C at P > 1.3 GPa for the M_1^E stage and T = ~630–680 °C at P = ~0.8–1.0 GPa for the M_1^A stage. The jadeite- and lawsonite-bearing phase equilibria constrain metamorphic conditions of P > 1.0 GPa at T = ~250–300 °C for the M_2 stage that is probably synchronous with the formation of nearby jadeitite within serpentinite. The presence of eclogite blocks suggests that the New Idria serpentinite diapir was initiated at mantle depths. The wide range of *P-T* conditions of tectonic blocks supports the idea that the New Idria serpentinite diapir rose from mantle depths and enclosed tectonic blocks at various mantle-crustal levels during diapiric upwelling and extrusion.

Keywords: serpentinite diaper, tectonic block, HP metamorphism, P-T path, Diablo Range.

†Present address: The Pheasant Memorial Laboratory for Geochemistry and Cosmochemistry, Institute for Study of the Earth's Interior, Okayama University, Misasa, Tottori 682-0193, Japan; e-mail: tatsukix@misasa.okayama-u.ac.jp.

Tsujimori, T., Liou, J.G., and Coleman, R.G., 2007, Finding of high-grade tectonic blocks from the New Idria serpentinite body, Diablo Range, California: Petrologic constraints on the tectonic evolution of an active serpentinite diapir, *in* Cloos, M., Carlson, W.D., Gilbert, M.C., Liou, J.G., and Sorensen, S.S., eds., Convergent Margin Terranes and Associated Regions: A Tribute to W.G. Ernst: Geological Society of America Special Paper 419, p. 67–80, doi: 10.1130/2007.2419(03).

INTRODUCTION

Serpentinite diapirism has been documented in many present-day forearc environments. For example, in the Izu-Bonin-Mariana interoceanic island arcs, numerous serpentinite seamounts are widely distributed (e.g., Fryer et al., 1995; Ishii et al., 1992; Kamimura et al., 2002; Miura et al., 2004; Seno, 2005). Some of these contain exotic blocks of blueschist- and eclogite-facies rock (Maekawa et al., 1993; Ueda et al., 2004), which suggests that serpentinite diapiric ascent may play a significant role in the exhumation of high-pressure metamorphic rocks, consistent with the common association of high-pressure blocks with serpentinite in many blueschist terranes. The on-land analogue of such active serpentinite diapirs has long been recognized in the New Idria serpentinite body of the California Coast Ranges (Coleman, 1961, 1986, 1996). The New Idria serpentinite contains jadeitite, and its exposure since at least middle Miocene time is indicated by clastic serpentinite debris in the Big Blue Formation (Coleman, 1961; Casey and Dickinson, 1976; Bate, 1985). The record of serpentinite erosion is verified by the presence of detrital serpentinites in Pliocene-Quaternary sediments. The presence of active landslides on the flanks of the New Idria serpentinite body (Cowan, 1979) and the deposition of detrital serpentinite in terrace deposits as young as 500 yr B.P. (Atwater et al., 1989) are also strong evidence that the New Idria serpentinite continues to rise. Moreover, recent fission track thermochronology from the Great Valley Group forearc

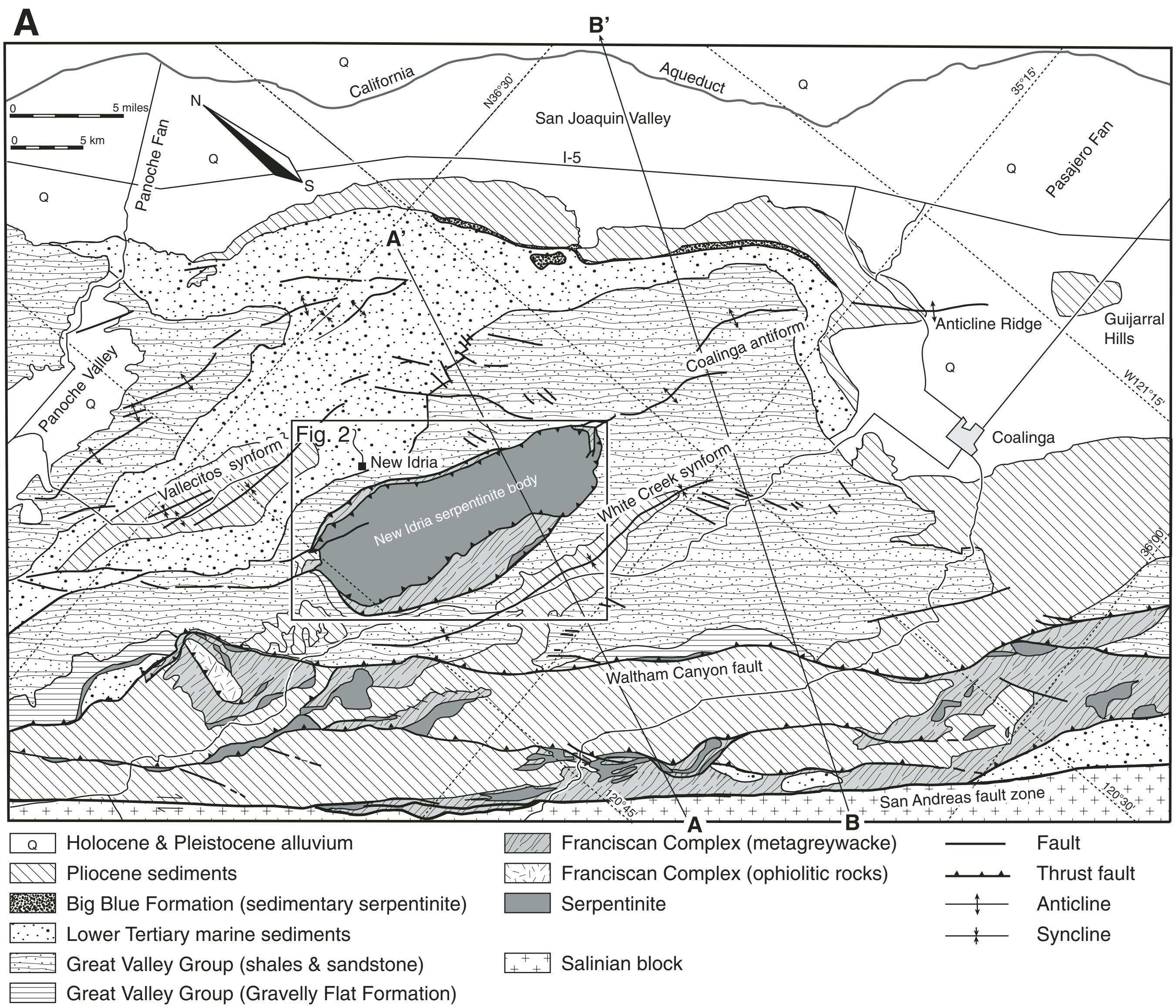

Figure 1 (*on this and following page*). Geologic map of the New Idria serpentinite body and surrounding area in the southern Diablo Range. The serpentinite body occupies the crest of the Coalinga antiform, and the high-angle normal faults surrounding it mark the exhumed trace of the Coast Range fault. B–B′ is modified after Namson et al. (1989). Note that cross sections do not match exactly the map since they are compiled from different maps.

sediments suggested the rapid rise of the New Idria serpentinite diapir as a heat source ($T > \sim 110$ °C) to anneal apatite fission tracks at ca. 14 Ma (Vermeesch et al., 2006). Although blocks of low-grade blueschist, jadeitite, greenstone and many other metasomatic rocks have been previously reported in the New Idria serpentinite body (e.g., Coleman, 1961, 1986; Van Baalen, 2004), we recently discovered high-grade blocks of eclogites and garnet-amphibolite near the jadeitite locality of Coleman (1961).

In this paper, we describe detailed petrologic and mineralogic characteristics of these high-grade blocks, and constrain the initiation of the New Idria serpentinite diapir. We also document possible origin of the New Idria serpentinite based on available petrotectonic data on ophiolitic rocks in the California continental margin and geophysical data for modern subduction zones. This is the first comprehensive petrologic report dealing with mafic tectonic blocks from one of the largest serpentinite bodies in the California Coast Ranges.

Mineral abbreviations are after Kretz (1983); we also use sodic amphibole (Na-amp), phengite (Phe), and aegirine (Ae) throughout this paper. The term "hornblende" (Hbl) is used to described Ca-amphibole with dominantly tschermakitic and edenitic composition. Abbreviations for element-sites are: [6]—octahedral M2-sites; [B]—decahedral B-sites of amphibole; [A]—10-coordinated A-site of amphibole.

GEOLOGIC SETTING

The New Idria serpentinite body (23 × 8 km) forms the core of the Coalinga antiform along the crest of the Diablo Range between the San Andreas fault on the west and the San Joaquin Valley on the east (Fig. 1). Tertiary and Mesozoic marine sedimentary rocks that surround the dome are folded into a series of anticlines and synclines that trend N70°W, oblique to the northwest trend of the San Andreas fault. These flanking sediments and the serpentinite body together comprise an asymmetric actively growing anticline that is the northern extension of the Coalinga anticline (Dibblee, 1972; Nilsen, 1984; Namson et al., 1989; Dickinson, 2002). The New Idria serpentinite is in contact with the Franciscan Complex and Upper Cretaceous Panoche and Moreno Formations of the Great Valley Group (Coleman, 1986; Vermeesch et al., 2006). The contact is marked by high-angle faults and shear zones that indicate upward differential movement of the New Idria serpentinite body (Coleman, 1980, 1996). The northeastern contact along the body has been called a thrust,

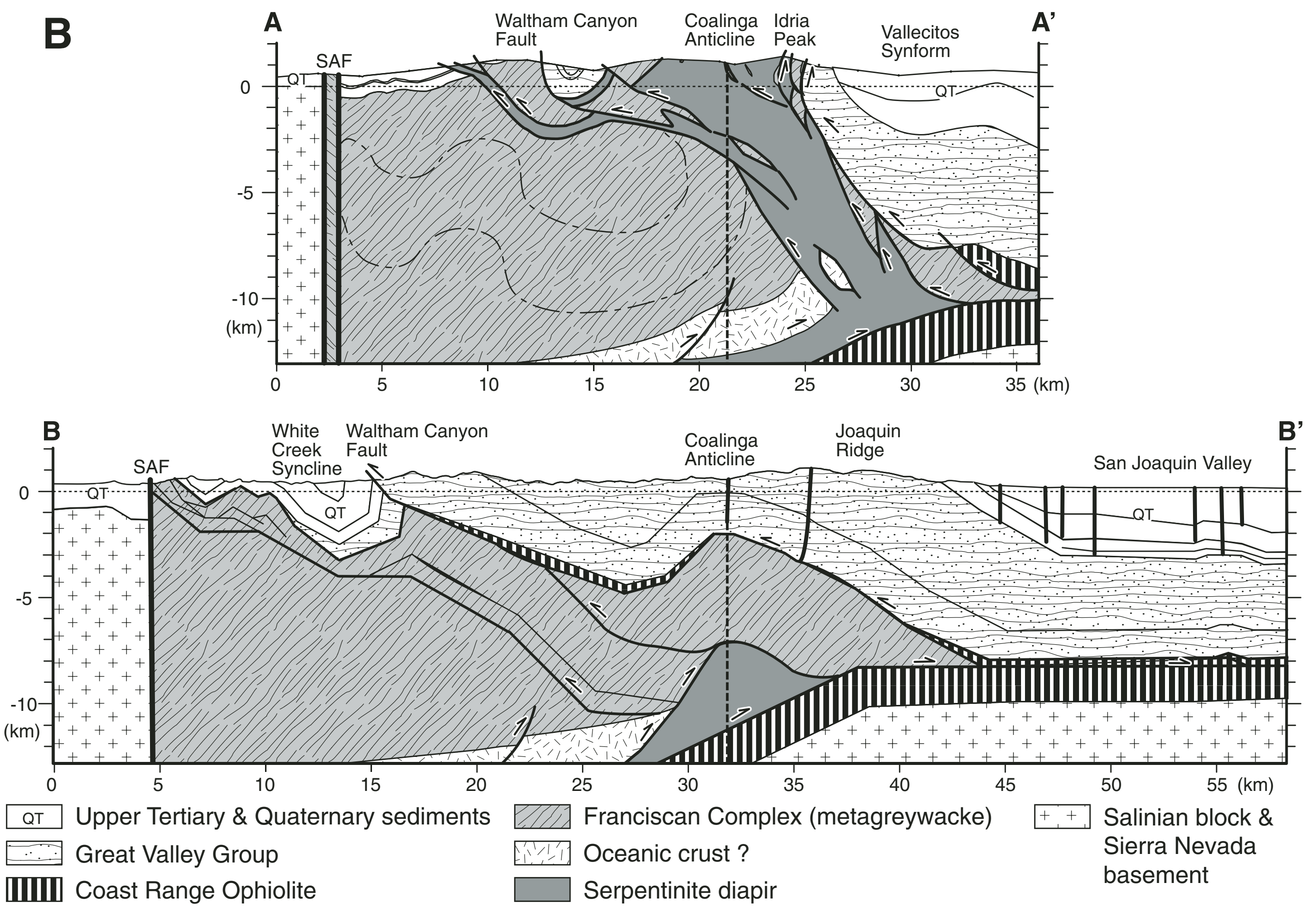

Figure 1 (*continued*). SAF—San Andreas fault.

as the subjacent Mesozoic and Tertiary sediments are overturned to the east by emplacement of the expanding serpentinite protrusion (Coleman, 1961; Eckel and Myers, 1946). The vertical displacement between the trough of the syncline and the patch of sediments on the crest of the serpentinite is 853 m, yielding an uplift rate of ~4 mm/yr during the Pliocene (Coleman, 1996).

The New Idria serpentinite body consists mainly of chrysotile-lizardite serpentinite and minor antigorite serpentinite. Only a few serpentinite samples preserve relict primary minerals including olivine (Fo_{91}), orthopyroxene (2.1–2.3 wt% Al_2O_3), clinopyroxene (1.6–2.2 wt% Al_2O_3), and chromian spinel (Cr/(Cr + Al) atomic ratio = 0.52–0.54). Compositions of these relict minerals suggest that the serpentinite was a moderately depleted harzburgite (Dick and Bullen, 1984; Arai, 1994) resembling some of the less serpentinized peridotites of the California Coast Ranges (Loney et al., 1971; Huot and Maury, 2002). A small syenite plug intruded the southern part of the New Idria serpentinite body during the middle Miocene (ca. 12 Ma), producing hydrothermal alteration in restricted zones in the serpentinite and its tectonic inclusions (Coleman, 1961; Johnson and O'Neil, 1984; Laurs et al., 1997; Obradovich et al., 2000; Van Baalen, 2004) (Fig. 2). This hydrothermal alteration produced an unique suite of titanium-rich minerals including the famous California State gem, benitoite, that has been dated at 12 Ma (e.g., Laurs et al., 1997; Obradovich et al., 2000).

The New Idria serpentinite contains numerous tectonic blocks of greenstone and low-grade blueschist up to 1500 m in length, and others less than a meter in diameter (Coleman, 1961, 1980) (Fig. 2). The blocks have a random distribution within the serpentinite body, and their internal metamorphic fabrics are disparate from block to block. The blocks are characteristically surrounded by sheared antigorite serpentinite in contrast to the main body that consists of chrysotile-lizardite (Fig. 2). Along Clear Creek, Coleman (1961) found blocks of monomineralic jadeitite rocks and jadeitite veins cutting low-grade blueschist blocks. The investigated high-grade blocks were found as river float near the jadeitite locality in Clear Creek (Fig. 2). As the headwaters for the Clear Creek drainage lie entirely within the serpentinite, the high-grade blocks must have come out of the serpentinite.

PETROGRAPHY

The high-grade blocks are extensively retrograded, but primary eclogite- or garnet-amphibolite mineral assemblages are locally preserved. Three rock types are recognized from the relict assemblages: (1) jadeite-bearing retrograded eclogite (JEC), (2) pumpellyite-rich retrograded eclogite (PEC), and (3) clinopyroxene-bearing garnet-amphibolite (CGA). Their lithologic and petrographic features are described below:

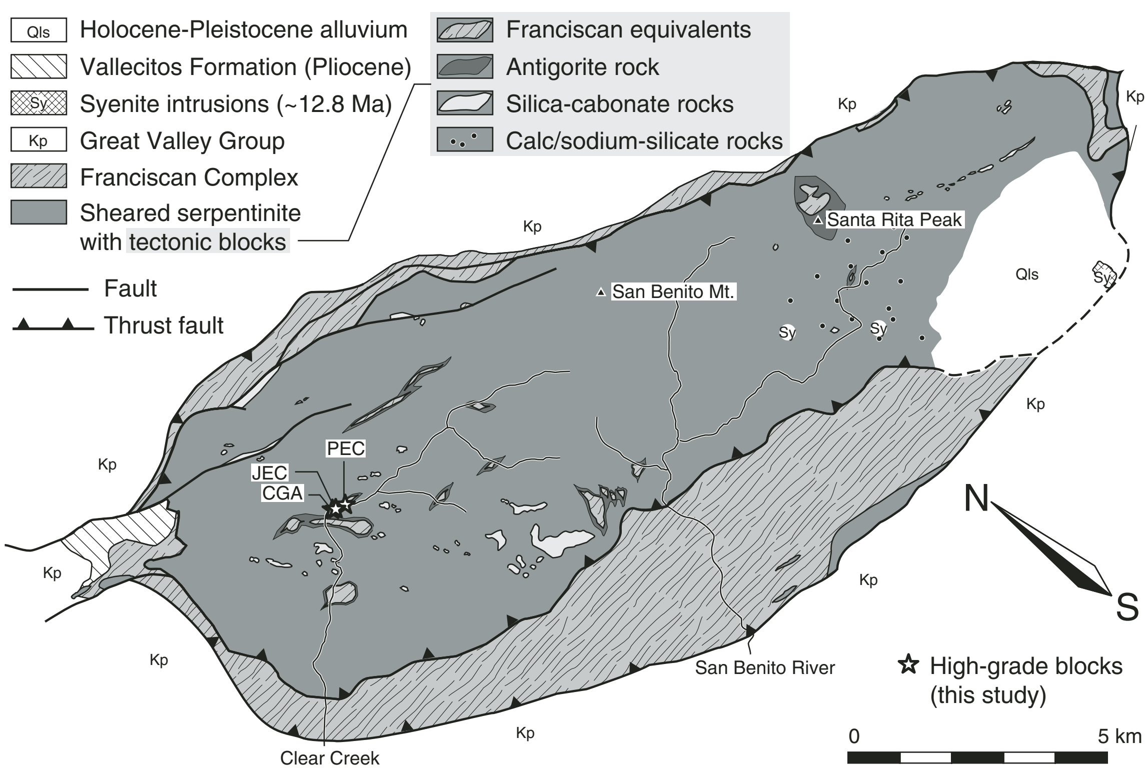

Figure 2. Detailed map of New Idria serpentinite body showing distribution of various tectonic blocks and syenite intrusions. The high-grade rock boulders were found only as alluvial materials in Clear Creek. JEC—jadeite-bearing retrograded eclogite; PEC—pumpellyite-rich retrograded eclogite; CGA—clinopyroxene-bearing garnet-amphibolite.

Jadeite-Bearing Retrograded Eclogite (JEC)

The JEC is a subrounded boulder (~30 cm in size). Chloritized garnet and pale-greenish omphacite-rich matrix are visible on the well-polished surface. Thin-section observation indicates that the specimen is a coarse-grained, massive metabasite characterized by unusually abundant chloritized garnet (up to 77 vol%) (Fig. 3A). Compositional banding (2–4 cm in thickness) is defined by varying amounts of garnet together with omphacite. Rare glaucophane-rich hydrous veins (~5 mm wide) crosscut the banding. Accessory minerals include sodic amphibole, jadeite, lawsonite, pumpellyite, chlorite, titanite, phengite, rutile, and apatite. Garnet is subhedral to anhedral (0.5–3 mm in size) and intensely chloritized along internal cracks (Fig. 3A). The chloritized garnets contain mineral inclusions of rutile, omphacite, and rare quartz and clinozoisite. Some internal fractures of garnet are filled by lawsonite. Omphacite occurs as aggregates of fine-grained crystals (less than 0.1 mm) in contact with garnet (Fig. 3B). Omphacite is replaced partly by retrograde jadeite, pumpellyite, and chlorite (Figs. 3C and 3D). In some cases, jadeite-poor clinopyroxene occurs as patches or as lamellae in omphacite. Retrograde jadeite occurs as irregularly shaped crystals associated with pumpellyite and chlorite and fills grain boundaries of omphacites (Fig. 3C); some retrograde jadeite contains mineral inclusions of pumpellyite. Titanite replacing rutile is ubiquitous in the matrix and contains mineral inclusions of sodic amphibole, chlorite, and pumpellyite. The mineral assemblage Grt + Omp ± Czo + Rt + Qtz is interpreted as the primary mineral assemblage representing a peak eclogite-facies metamorphism, whereas the assemblage Na-amp + Jd + Pmp + Lws + Chl + Ttn ± Phe formed during blueschist-facies retrogression.

Pumpellyite-Rich Retrograded Eclogite (PEC)

The PEC is a well-polished, dark-greenish rounded boulder (~60 cm in size); garnet pseudomorphs are barely visible by hand lens. The PEC is a highly retrograded, fine-grained eclogite. It consists mainly of omphacite (46%), chloritized garnet (19%), chlorite (20%), pumpellyite (11%), minor amounts of titanite, and rare lawsonite. Chloritized garnet preserves its euhedral shape (0.5–1.2 mm in size) (Fig. 3E). Internal fractures of garnet are filled by lawsonite. Clinozoisite and apatite are present as trace tiny inclusions in garnet. Omphacite occurs as radial aggregates of fine-grained crystals. It commonly contains irregularly shaped patches or lamellae of diopside (Fig. 3F). Omphacite aggregates are replaced by chlorite and pumpellyite. Pumpellyite occurs as randomly oriented colorless prisms (up to 2 mm in length) in the matrix (Fig. 3G), and as green fibrous aggregates (<0.5 mm) included in chloritized garnet. Rutile is rare in the core of titanite (Fig. 3H). The mineral assemblage Grt + Omp + Rt ± Czo + Qtz characterizes the peak eclogite-facies metamorphism, whereas the assemblage Pmp + Lws + Chl + Ttn reflects the blueschist-facies overprinting.

Clinopyroxene-Bearing Garnet-Amphibolite (CGA)

The CGA is a dark-colored gneissic cobble (~20 cm in size). The CGA consists mainly of hornblende, chloritized garnet, and diopsidic clinopyroxene with minor titanite, chlorite, sodic amphibole, pumpellyite, quartz, and rare jadeite and rutile. Apatite and rare tourmaline are accessories. A weak foliation is defined by oriented granonematoblastic hornblende grains. Hornblende (<1.5 mm in length) shows pale-brownish pleochroic color. Bluish glaucophane overgrows the margins and fills internal cracks of the hornblende. Subhedral to euhedral garnet, up to 1 mm diameter, contains inclusions of clinopyroxene and rare quartz and is moderately chloritized. Some finer garnets (<0.5 mm in size) are included in hornblende and clinopyroxene (Fig. 3I). Clinopyroxene occurs as granoblasts (<1.5 mm in length) and is partly replaced by pumpellyite, chlorite, and rare jadeite along cleavages. Secondary titanite associated with chlorite is ubiquitous in the matrix; rare rutile was found in titanite cores. The metamorphic peak is characterized by a primary matrix assemblage of Grt + Hbl + Cpx + Qtz + Rt; the secondary mineral assemblage of Gln + Pmp + Chl ± Jd + Ttn represents a blueschist-facies retrogression.

MINERAL CHEMISTRY

Electron microprobe analysis was carried out with a JEOL JXA-8900R at Okayama University of Science. Quantitative analyses of both peak and retrograde minerals were performed with 15 kV accelerating voltage, 12 nA beam current, and 3–5 μm beam size. Natural and synthetic silicates and oxides were used as standards for calibration. The CITZAF method (Armstrong, 1988) was employed for matrix corrections. Representative analyses are listed in Tables 1, 2, and 3.

Garnet

Compositions of garnets of each rock type are plotted in the three binary diagrams X_{Mg}-alm, X_{Mg}-sps, and X_{Mg}-grs, where X_{Mg} = Mg/(Mg + Fe), alm = 100 × Fe/(Fe + Mn + Mg + Ca), sps = 100 × Mn/(Fe + Mn + Mg + Ca), and grs = 100 × Ca/(Fe + Mn + Mg + Ca) (Fig. 4). Garnets in the JEC are rich in almandine (alm) component with moderate grossular (grs) and pyrope (prp) and very low spessartine (sps) ($alm_{50–62}grs_{22–32}prp_{12–17}sps_{<3}$); X_{Mg} ranges from 0.17 to 0.25. These garnets show prograde chemical zoning: X_{Mg} increases from core to rim; grossular component slightly increases rimward. Garnets in the PEC have compositions of $alm_{48–57}grs_{29–36}prp_{9–17}sps_{1–8}$; grossular and spessartine components are slightly higher than in garnets from the JEC. The X_{Mg} increases rimward (X_{Mg} = 0.15–0.26), indicating prograde growth. Garnets in the CGA are characterized by markedly higher grossular compositions ($alm_{45–50}grs_{34–41}prp_{8–15}sps_{1–7}$) than those from other rock types. As in the other two samples, the X_{Mg} increases from core to rim (X_{Mg} = 0.14–0.25).

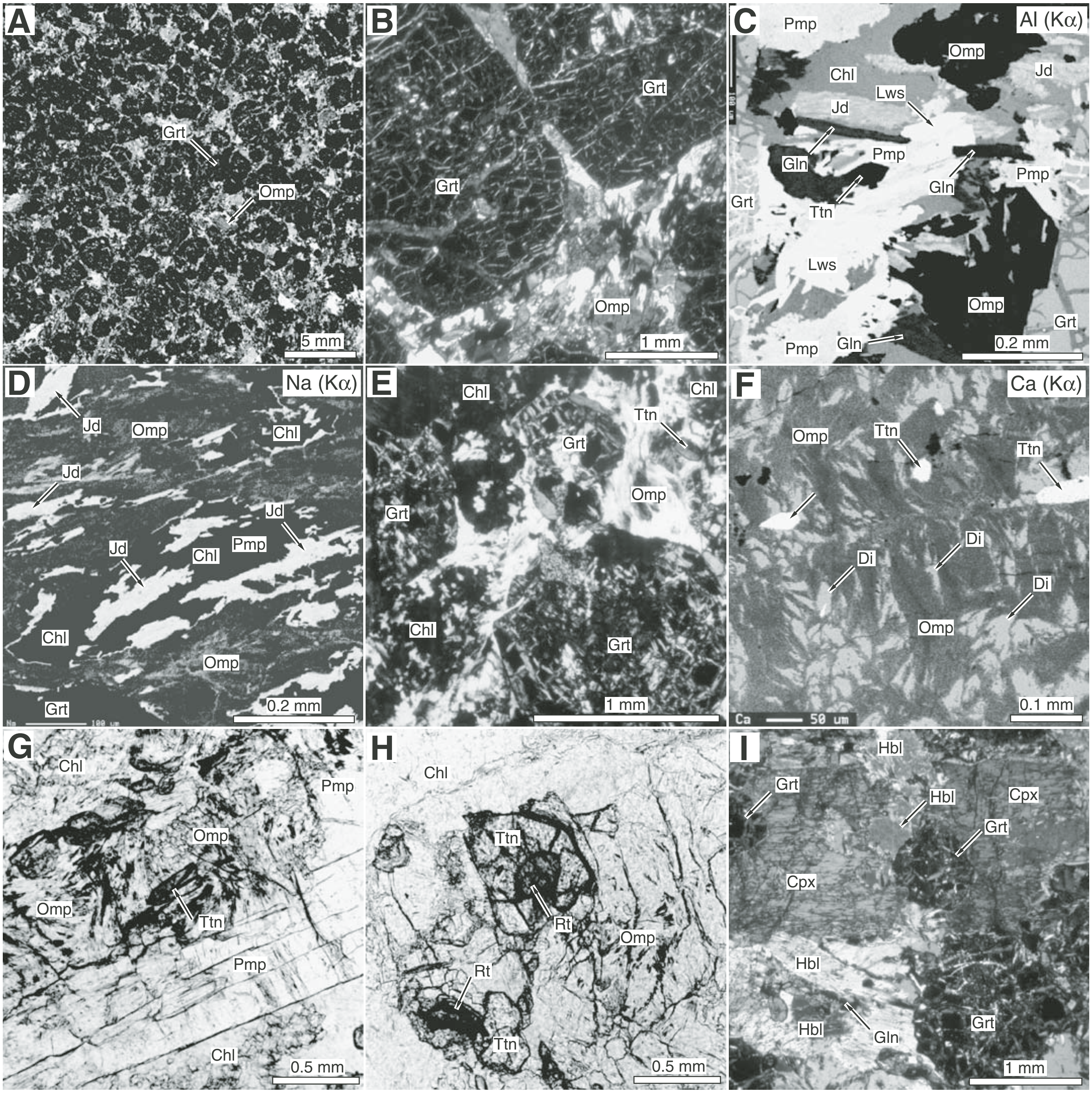

Figure 3. Microtextures of the investigated high-grade rocks in the New Idria serpentinite body. (A) Photomicrograph showing garnet-rich matrix of the JEC (cross-polarized light). (B) Porphyroblastic garnets (Grt) of the JEC (cross-polarized light). (C) X-ray image of Al (*K*α) of retrograde minerals of the JEC. Garnets are fractured and matrix omphacites are replaced by chlorite (Chl), jadeite (Jd), lawsonite (Lws), pumpellyite (Pmp), and glaucophane (Gln). (D) X-ray image of Na (*K*α) of matrix omphacite of the JEC. Omphacite is partly replaced by various secondary minerals including jadeite. (E) Chloritized porphyroblastic garnets of the PEC (cross-polarized light). (F) X-ray image of Ca (*K*α) of matrix omphacite of the PEC. Omphacite contains irregularly shaped patches and lamellae of diopside. (G) Prismatic pumpellyite of the PEC (plane-polarized light). (H) Rutile preserved in the titanite cores of the PEC (plane-polarized light). (I) Photomicrograph showing granonematoblastic diopsidic pyroxene (Cpx) of the CGA. Clinopyroxene contains garnet and hornblende inclusions.

TABLE 1. REPRESENTATIVE ELECTRON-MICROPROBE ANALYSES OF ROCK-FORMING MINERALS IN THE JEC

	Garnet		Omphacite			Ep	Jd	Na-amp	Lws	Pmp	Phe
	core	rim				M_1^E	M_2	M_2	M_2	M_2	M_2
			Inc		Exs						
SiO_2	38.31	38.26	55.20	55.31	53.82	37.94	58.70	56.49	38.24	37.10	52.35
TiO_2	0.08	0.09	0.10	0.02	0.00	0.45	0.09	0.03	0.06	0.20	0.05
Al_2O_3	21.01	21.18	7.90	8.33	2.21	26.03	21.97	10.67	31.44	24.73	25.28
Cr_2O_3	0.03	0.12	0.25	0.06	0.01	0.12	0.09	0.10	0.05	0.09	0.11
FeO*	27.49	23.74	9.67	8.36	11.31	9.11	3.06	14.22	0.56	3.93	3.74
MnO	0.78	0.75	0.23	0.12	0.22	0.00	0.02	0.09	0.00	0.29	0.05
MgO	3.39	4.21	6.60	6.91	9.65	0.12	0.35	7.32	0.00	2.99	3.41
CaO	9.34	11.04	12.78	13.50	19.91	23.44	0.55	0.76	17.35	22.51	0.00
Na_2O	0.01	0.04	7.09	7.02	2.92	0.03	15.22	7.21	0.00	0.19	0.16
K_2O	0.00	0.00	0.00	0.01	0.00	0.00	0.00	0.03	0.01	0.00	9.51
Total	100.44	99.43	99.82	99.64	100.05	97.24	100.05	96.92	87.71	92.02	94.64
O =	12	12	6	6	6	12.5	6	23	8	24.5	11
Si	3.012	3.003	2.001	1.999	2.004	2.996	1.999	7.978	2.021	6.035	3.510
Ti	0.005	0.006	0.003	0.001	0.000	0.027	0.002	0.004	0.003	0.025	0.003
Al	1.947	1.959	0.338	0.355	0.097	2.422	0.882	1.776	1.958	4.741	1.997
Cr	0.002	0.008	0.007	0.002	0.000	0.008	0.002	0.011	0.002	0.011	0.006
Fe^{3+}			0.146	0.137	0.106	0.542	0.087	0.041	0.020		
Fe^{2+}	1.807	1.558	0.147	0.116	0.246		0.000	1.638		0.535	0.210
Mn	0.052	0.050	0.007	0.004	0.007	0.000	0.001	0.011	0.000	0.040	0.003
Mg	0.397	0.493	0.357	0.372	0.535	0.014	0.018	1.541	0.000	0.725	0.340
Ca	0.787	0.928	0.496	0.523	0.794	1.983	0.020	0.115	0.982	3.923	0.000
Na	0.001	0.005	0.498	0.492	0.211	0.004	1.005	1.974	0.000	0.059	0.020
K	0.000	0.000	0.000	0.000	0.000	0.000	0.000	0.005	0.001	0.000	0.813
Total	8.010	8.010	4.000	4.000	4.000	7.994	4.016	15.094	4.987	16.094	6.903
X_{Mg}	0.18	0.24	0.71	0.76	0.69		1.00	0.48		0.58	0.62

Note: FeO* = total Fe as FeO. X_{Mg} = Mg/(Mg + Fe^{2+}). Ep—Epidote; Exs—exsolution; Inc—inclusion in garnet; Jd—Jadeite; JEC—jadeite-bearing retrograded eclogite; Lws—Lawsonite; M1—M_1^E; M_2—blueschist-facies overprinting; Na-amp—Na-amphibole; Phe—Phengite; Pmp—Pumpellyite.

TABLE 2. REPRESENTATIVE ELECTRON-MICROPROBE ANALYSES OF ROCK-FORMING MINERALS IN THE PEC

	Garnet		Omphacite			Ep	Pumpellyite		Lws
	core	rim	Omp	Omp w/Exs	Di Exs	M1	M_2 P	M_2 F	M_2
SiO_2	38.49	38.48	55.93	56.48	53.02	40.04	38.73	37.76	37.48
TiO_2	0.14	0.08	0.18	0.08	0.01	0.12	0.00	0.09	0.03
Al_2O_3	21.66	21.81	9.70	10.65	0.47	27.84	26.59	24.09	25.13
Cr_2O_3	0.00	0.07	0.02	0.05	0.00	0.00	0.03	0.02	0.11
FeO*	25.38	22.56	6.57	5.20	12.36	5.39	2.55	6.20	2.85
MnO	0.97	0.66	0.05	0.00	0.06	0.26	0.29	0.00	0.12
MgO	2.80	4.27	6.90	7.01	11.08	0.22	3.07	1.15	3.25
CaO	11.28	11.92	13.97	12.65	22.42	23.64	22.25	22.06	22.66
Na_2O	0.04	0.03	6.99	7.69	0.65	0.05	0.30	0.17	0.15
K_2O	0.00	0.00	0.00	0.00	0.00	0.00	0.01	0.02	0.00
Total	100.77	99.89	100.31	99.82	100.06	97.56	93.81	91.55	91.78
O =	12	12	6	6	6	12.5	24.5	24.5	24.5
Si	3.002	2.992	2.000	2.010	2.005	3.087	6.099	6.209	2.036
Ti	0.008	0.005	0.005	0.002	0.000	0.007	0.000	0.011	0.006
Al	1.991	1.999	0.409	0.447	0.021	2.529	4.934	4.669	1.884
Cr	0.000	0.004	0.000	0.001	0.000	0.000	0.004	0.003	0.000
Fe^{3+}			0.065	0.058	0.016	0.347			0.037
Fe^{2+}	1.656	1.467	0.131	0.097	0.375		0.336	0.853	
Mn	0.064	0.044	0.002	0.000	0.002	0.017	0.039	0.000	0.001
Mg	0.325	0.495	0.368	0.372	0.625	0.025	0.719	0.282	0.021
Ca	0.943	0.993	0.535	0.482	0.908	1.952	3.754	3.888	1.012
Na	0.006	0.005	0.485	0.531	0.048	0.007	0.093	0.054	0.004
K	0.000	0.000	0.000	0.000	0.000	0.000	0.002	0.004	0.000
Total	7.997	8.004	4.000	4.000	4.000	7.972	15.980	15.972	5.000
X_{Mg}	0.16	0.25	0.74	0.79	0.62		0.68	0.25	

Note: FeO* = total Fe as FeO. X_{Mg} = Mg/(Mg + Fe^{2+}). Inc—inclusion in garnet; Ep—Epidote; Exs—exsolution (w/Exs—host); F—fibrous; Jd—Jadeite; Lws—Lawsonite; M1—M_1^E; M_2—blueschist-facies overprinting; Na-amp—Na-amphibole; P—prismatic; PEC—pumpellyite-rich retrograded eclogite; Phe—Phengite; Pmp—Pumpellyite.

TABLE 3. REPRESENTATIVE ELECTRON-MICROPROBE ANALYSES OF ROCK-FORMING MINERALS IN THE CGA

	Garnet		Clinopyroxene		Hbl	Jd	Na-amp	Pmp
	core	rim	M_1^A	M_1^A Inc	M_1^A	M_2	M_2	M_2
SiO_2	38.42	38.62	53.12	53.58	45.63	57.14	56.55	37.48
TiO_2	0.14	0.10	0.06	0.12	0.67	0.42	0.12	0.03
Al_2O_3	21.47	21.50	3.11	2.94	12.51	15.38	9.54	25.13
Cr_2O_3	0.00	0.02	0.06	0.00	0.15	0.08	0.04	0.11
FeO*	22.08	22.66	6.97	7.21	11.47	7.33	13.64	2.85
MnO	2.61	0.44	0.00	0.00	0.02	0.08	0.25	0.12
MgO	2.35	3.88	12.73	12.70	12.59	2.40	7.82	3.25
CaO	13.06	12.49	22.30	22.56	11.46	3.74	0.59	22.66
Na_2O	0.03	0.01	1.40	1.17	2.63	12.86	8.14	0.15
K_2O	0.00	0.00	0.01	0.00	0.24	0.00	0.06	0.00
Total	100.16	99.71	99.77	100.30	97.39	99.43	96.75	91.78
O =	12	12	6	6	23	6	23	24.5
Si	3.009	3.011	1.962	1.974	6.636	1.999	8.027	6.069
Ti	0.008	0.006	0.002	0.003	0.073	0.011	0.013	0.003
Al	1.982	1.976	0.135	0.128	2.145	0.634	1.597	4.796
Cr	0.000	0.001	0.002	0.000	0.018	0.002	0.005	0.014
Fe^{3+}			0.037	0.001	0.063	0.214	0.000	
Fe^{2+}	1.446	1.477	0.179	0.221	1.332	0.000	1.619	0.386
Mn	0.173	0.029	0.000	0.000	0.003	0.002	0.030	0.017
Mg	0.274	0.451	0.701	0.698	2.730	0.125	1.654	0.784
Ca	1.096	1.043	0.882	0.891	1.786	0.140	0.089	3.931
Na	0.005	0.002	0.100	0.084	0.740	0.872	2.240	0.046
K	0.000	0.000	0.001	0.000	0.044	0.000	0.011	0.000
Total	7.994	7.996	4.000	4.000	15.570	4.001	15.285	16.046
X_{Mg}	0.16	0.23	0.80	0.76	0.67	1.00	0.51	0.67

Note: FeO* = total Fe as FeO. X_{Mg} = Mg/(Mg + Fe^{2+}). CGA—clinopyroxene-bearing garnet-amphibolite; Hbl—Hornblende; M_1^A—amphibolite-facies metamorphism; M_2—blueschist-facies overprinting; Inc—inclusion in garnet.

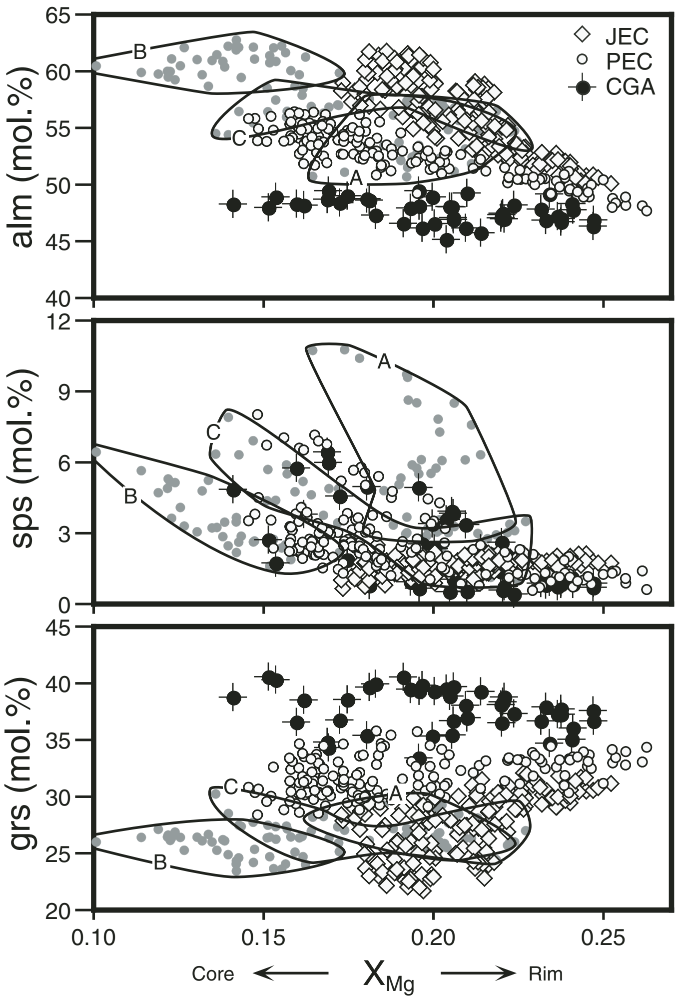

Figure 4. Compositions of analyzed garnets on alm, sps, and grs components versus X_{Mg}. For comparisons, garnets from the Tiburon eclogite are also plotted; solid lines represent individual samples A, B, and C of Tsujimori et al. (2006a). JEC—jadeite-bearing retrograded eclogite; PEC—pumpellyite-rich retrograded eclogite; CGA—clinopyroxene-bearing garnet-amphibolite.

Clinopyroxenes

Clinopyroxene analyses are plotted in the jd–aug (di + hd)–ae ternary diagram (Fig. 5). The Fe^{2+}/Fe^{3+} ratio and end-member components of sodic pyroxene were calculated by an algorithm suggested by Harlow (1999). Analyzed clinopyroxenes are nearly free of Ca-Tschermak component except for those from the CGA. Omphacites in the JEC have compositions of $jd_{27–38}aug_{48–58}ae_{3–18}$, with X_{Mg} = 0.57–0.76. Exsolution lamellae in the JEC omphacite are $jd_{10–18}aug_{67–80}ae_{10–15}$, with X_{Mg} = 0.59–0.71. Retrograde jadeites in the JEC are nearly binary jadeite-aegirine compositions of $jd_{70–94}aug_{1–6}ae_{3–24}$; the jd component is comparable to jadeitite in monomineralic jadeitite in the New Idria serpentinite and is remarkably higher than those from the New Idria lawsonite-blueschist (Fig. 5). Omphacites in the PEC have compositions of $jd_{38–47}aug_{45–55}ae_{2–11}$, X_{Mg} = 0.70–0.79, and show a wide compositional gap between their host and diopside lamellae ($jd_{1–5}aug_{87–96}ae_{0–6}$; X_{Mg} = 0.61–0.67). Diopsidic clinopyroxenes in the CGA contains up to 4 mol% Ca-Tschermak component and is characterized by low-jd and -ae components ($jd_{4–13}aug_{83–89}ae_{0–6}$; X_{Mg} = 0.75–0.85). Retrograde jadeites replacing primary clinopyroxenes have compositions of $jd_{60–65}aug_{14–19}ae_{18–21}$, with X_{Mg} > 0.87.

Amphiboles

The structural formulae of amphiboles are calculated based on O = 23; the Fe^{2+}/Fe^{3+} ratio was estimated based on total cations = 13 excluding Ca, Na, and K (Leake et al., 1997). Analyzed amphiboles are plotted in two binary diagrams, $^{[4]}Al$-$^{[B]}Na$ and $^{[4]}Al$-($^{[A]}Na$ + $^{[A]}K$) (Fig. 6). All retrograde sodic amphiboles in the JEC and CGA are glaucophane or ferroglaucophane with X_{Mg} = 0.37–0.54 and $Fe^{3+}/(Fe^{3+} + {}^{[6]}Al) < 0.13$. Primary hornblendes in the CGA have edenitic to tschermakitic compositions with $^{[B]}Na$ = 0.12–0.31, $^{[A]}Na + {}^{[A]}K$ = 0.41–0.61, and X_{Mg} = 0.66–0.72; they contain up to 13 wt% Al_2O_3, 2.5 wt% Na_2O, and 0.68 wt% TiO_2.

Other Minerals

Epidote inclusions in garnets of the JEC and PEC are characterized by relatively low $Fe^{3+}/(Fe^{3+} + Al)$ ratios (0.11–0.18). Lawsonites in the JEC and PEC contain 0.4–1.4 wt% Fe_2O_3. Pumpellyites in the JEC are characterized by high Al/(Al + Mg + Fe) ratio (0.73–0.83); the X_{Mg} of prismatic pumpellyite (0.56–0.73)

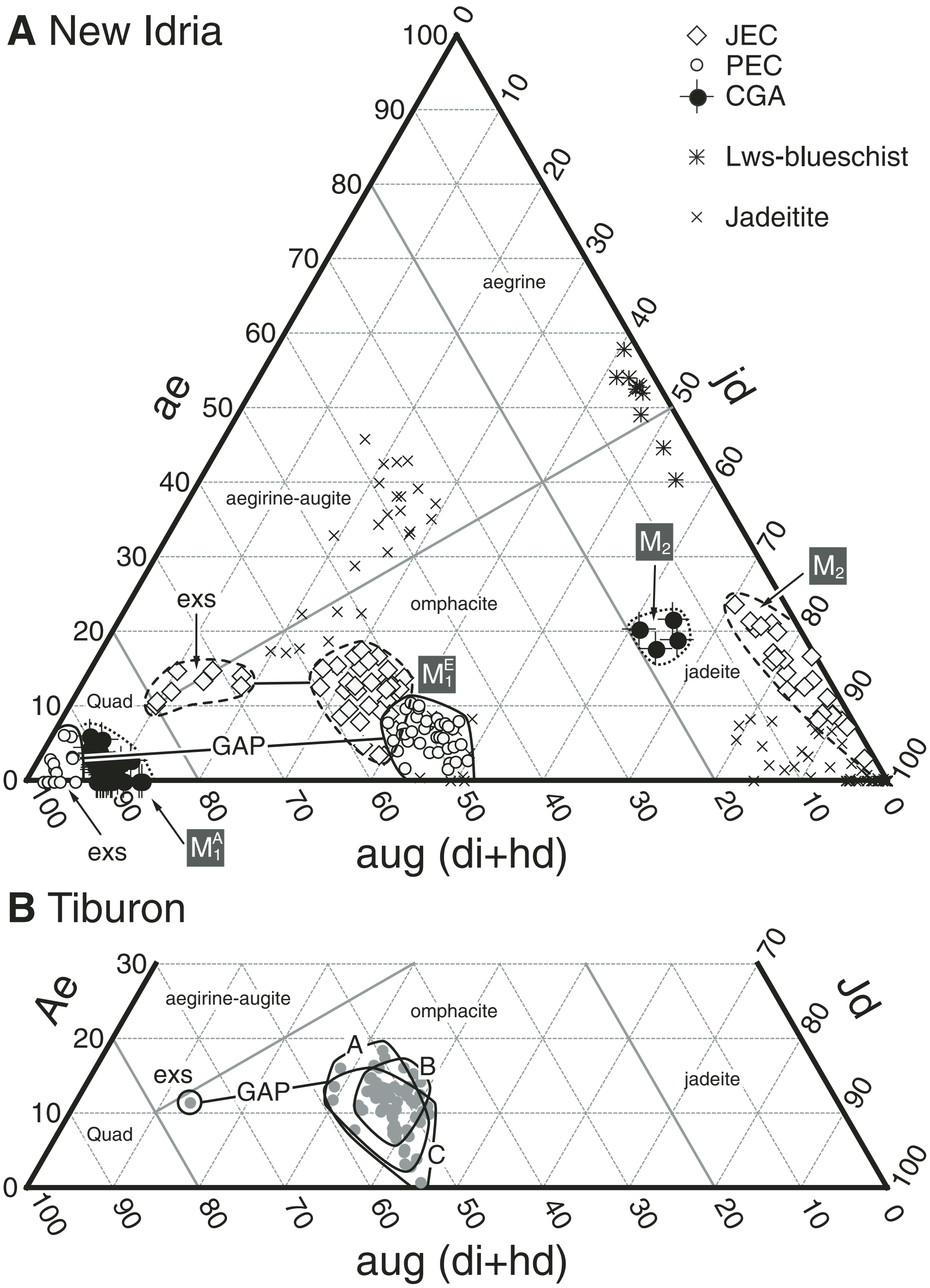

Figure 5. Compositions of analyzed clinopyroxenes on a jd-aug-ae ternary diagram. For comparisons, clinopyroxenes from lawsonite-blueschist and jadeitite blocks from the New Idria serpentinite body (A), and the Tiburon eclogite (B), are also plotted; solid lines represent individual samples A, B, and C of Tsujimori et al. (2006a). exs—exsolution lamella; quad—Quad end-member by Morimoto et al. (1988), gap—compositional gap. M_1^E—eclogite-facies metamorphism; M_1^A—amphibolite-facies metamorphism; M_2—blueschist-facies overprinting; JEC—jadeite-bearing retrograded eclogite; PEC—pumpellyite-rich retrograded eclogite; CGA—clinopyroxene-bearing garnet-amphibolite.

is higher than that of fibrous pumpellyite (0.18–0.43). Pumpellyites in the CGA are Al-rich (Al/(Al + Mg + Fe) = 0.80–0.81); X_{Mg} ranges from 0.61 to 0.68. Phengites in the JEC are Si-rich (3.4–3.5 Si p.f.u.); X_{Mg} ranges from 0.58 to 0.64. Titanites contain 1.1–1.8 wt% Al_2O_3 (JEC), 0.8–1.9 wt% Al_2O_3 (PEC), and 1.3–1.6 wt% Al_2O_3 (CGA).

P-T CONDITIONS OF METAMORPHISM

Based on observed petrographic features, compositions, and mineral parageneses, at least two different stages of metamorphic crystallization—peak eclogite-facies (M_1^E) or amphibolite-facies (M_1^A) and blueschist-facies overprinting (M_2)—are identified in each of the blocks. Mineral parageneses for different metamorphic stages of these rock types are summarized in Figure 7. The JEC and PEC record eclogite-facies metamorphism (M_1^E), whereas the CGA preserves amphibolite-facies metamorphism (M_1^A). Characteristic features for each stage are described below:

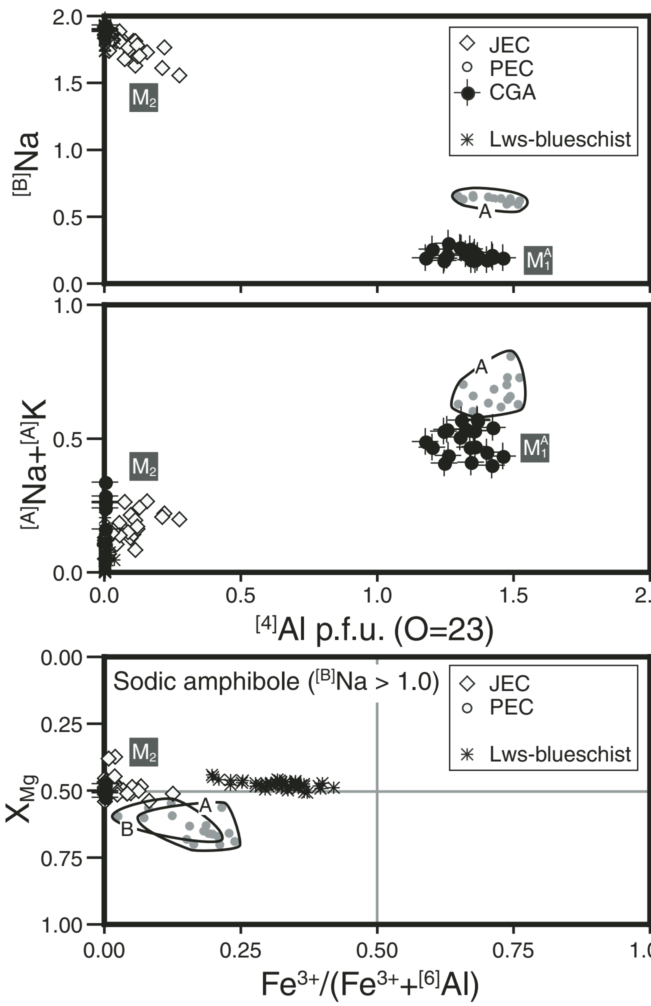

Figure 6. Compositions of analyzed amphiboles. For comparisons, amphiboles from lawsonite-blueschist block from the New Idria serpentinite body, and the Tiburon eclogite, are also plotted; solid lines represent individual samples A and B of Tsujimori et al. (2006a). M_1^A—amphibolite-facies metamorphism; M_2—blueschist-facies overprinting; JEC—jadeite-bearing retrograded eclogite; PEC—pumpellyite-rich retrograded eclogite; CGA—clinopyroxene-bearing garnet-amphibolite.

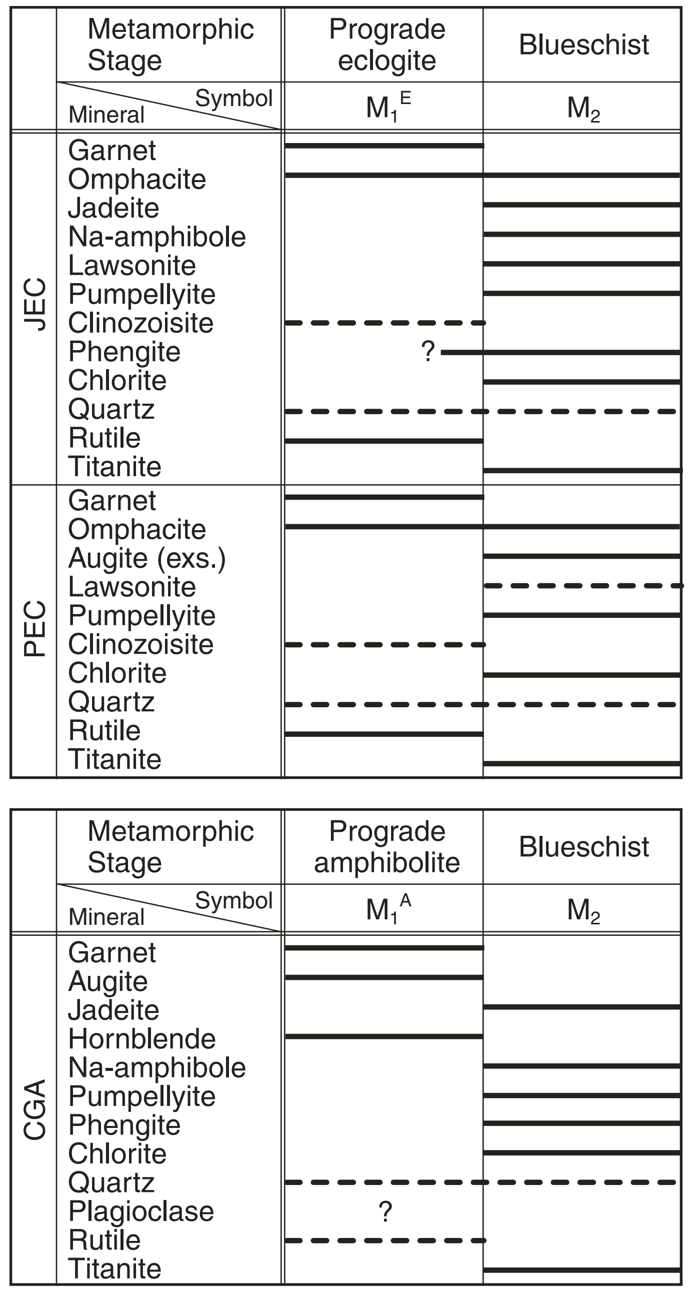

Figure 7. Mineral parageneses for the different stages of metamorphic recrystallization for the studied high-grade rocks. exs—exsolution lamella. M_1^E—eclogite-facies metamorphism; M_1^A—amphibolite-facies metamorphism; M_2—blueschist-facies overprinting; JEC—jadeite-bearing retrograded eclogite; PEC—pumpellyite-rich retrograded eclogite; CGA—clinopyroxene-bearing garnet-amphibolite.

Eclogite-Facies Metamorphism (M_1^E) in the JEC and PEC

The M_1^E mineral assemblage, Grt + Omp + Rt ± Czo + Qtz, in the JEC and PEC represents prograde eclogite-facies metamorphism. Prograde-zoned garnet with X_{Mg} increasing continuously from cores implies progressive increase in temperature during garnet growth. The thermal and probably the peak baric condition was achieved at the highest-X_{Mg} portion of the garnet rims. The Jd + Qtz sliding equilibrium (Holland, 1983) and Grt-Cpx thermometry (Krogh-Ravna, 2000) of the matrix omphacite (less exsolved part) and adjacent garnet rims of both JEC and PEC yield T = ~580–650 °C at a minimum P = 1.3 GPa for the eclogite-facies stage (Fig. 8).

Amphibolite-Facies Metamorphism (M_1^A) in the CGA

Amphibolite-facies metamorphism (M_1^A) produced the assemblage Grt + Cpx + Hbl + Rt + Qtz. The absence of omphacite and epidote, and the presence of diopsidic pyroxene ($jd_{\sim13}$) and brown hornblende, in the CGA suggest that M_1^A represents higher-T, lower-P conditions than the M_1^E assemblages in the JEC and PEC. The Jd + Qtz sliding equilibrium (Holland, 1983) and Grt-Cpx thermometry (Krogh-Ravna, 2000) of clinopyroxene and adjacent garnet give a P = 0.8–1.0 GPa at T = ~630–680 °C for the amphibolite-facies stage (Fig. 8). Moreover, the relatively high Al (up to 13 wt% Al_2O_3) and Ti (up to 0.7 wt% TiO_2) and moderate Na (up to 2.5 wt%) contents of hornblende, combined with the presence of rutile instead of titanite and ilmenite, further support these P-T estimates (Ernst and Liu, 1998; Liu et al., 1996).

Blueschist-Facies Overprinting (M_2)

The M_2 stage is characterized by blueschist-facies minerals that include sodic amphibole, jadeite, chlorite, pumpellyite, lawsonite, and titanite. The breakdown of rutile is critical to defining this later blueschist-facies recrystallization. The textural relations of these minerals suggest significant hydration of primary phases during M_2 metamorphism. M_2 minerals of all three rock types are interpreted as partial assemblages of Na-amp + Jd ($Jd_{\sim94}$) + Pmp + Lws + Chl + Ttn ± Phe (3.5 Si p.f.u.). This jadeite-bearing mineral assemblage is similar to those of common Franciscan low-grade blueschists and metagraywackes (e.g., Ernst, 1971; Banno et al., 2000), in particular the pumpellyite-zone metabasites in the Cazadero area, except for the lack of albite (e.g., Maruyama and Liou, 1987, 1988). Maruyama and Liou (1988) suggested a temperature range for pumpellyite-zone metabasites of T = 200–290 °C. The absence of albite suggests that M_2 minerals crystallized close to or within the Jd + Qtz stability field (P > 1.0 GPa) (Fig. 8). As described above, omphacites of the JEC and PEC characteristically contain lamellae of diopsidic pyroxene. Such omphacite-diopsidic (or augitic) pyroxene pairs are known to be stable at low-T blueschist-facies conditions; the compositional gap between omphacite and diopside becomes significantly wider

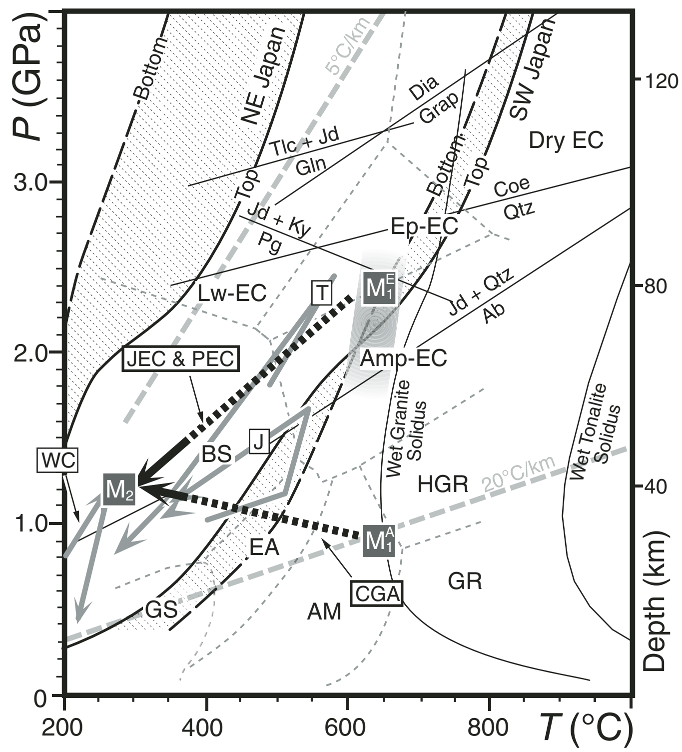

Figure 8. *P-T* diagrams showing a qualitative metamorphic condition of peak M_1^E (gray-gradiented area) and M_1^A stages, and retrograde *P-T* paths to M_2. The inferred *P-T* paths of exotic high-grade eclogite blocks (J—Jenner: Krogh et al., 1994; T—Tiburon: Tsujimori et al., 2006b) and coherent low-grade blueschist (WC—Ward Creek: Banno et al., 2000) from the Franciscan Complex are also shown (gray arrows). Hatched areas represent calculated *P-T* conditions of NE Japan ("cold") and SW Japan ("warm") subduction zones (Peacock and Wang, 1999); the solid and dashed lines show the top and bottom of oceanic crust. Metamorphic facies and their abbreviations, and phase equilibria, are after Liou et al. (2004). M_1^E—eclogite-facies metamorphism; M_1^A—amphibolite-facies metamorphism; M_2—blueschist-facies overprinting; JEC—jadeite-bearing retrograded eclogite; PEC—pumpellyite-rich retrograded eclogite; CGA—clinopyroxene-bearing garnet-amphibolite

with decreasing temperature (e.g., Tsujimori, 1997; Tsujimori and Liou, 2004); hence, diopside lamellae may have exsolved from eclogitic omphacite during the M_2 stage.

DISCUSSION

Petrologic Constraints on the Initiation of the New Idria Serpentinite Diapir

High-grade tectonic blocks within serpentinite- or shale-matrix mélange are one of the most characteristic features of the Franciscan Complex (e.g., Coleman and Lanphere, 1971; Brown and Bradshaw, 1979; Cloos, 1986; Moore and Black, 1989; Wakabayashi, 1990, 1999; Oh and Liou, 1990; Krogh et al., 1994; Anczkiewicz et al., 2004; Saha et al., 2005; Tsujimori et al., 2006a) and Santa Catalina Island (Sorensen, 1988). As we described, New Idria eclogites (JEC and PEC) do not contain eclogite-facies prograde amphibole (katophoritic/barroisitic or glaucophanic amphiboles), which occurs in most Franciscan eclogites (e.g., Krogh et al., 1994; Tsujimori et al., 2006a). The presence of abundant garnet (up to 77 vol%) in the JEC is also a unique characteristic. Compared with well-studied Franciscan eclogites, the inferred temperature condition of the New Idria eclogites is significantly higher than that of Franciscan eclogites (Fig. 8). Nevertheless, the presence of eclogite blocks in the New Idria serpentinite suggests that the New Idria serpentinite diapir was initiated at mantle depths and enclosed eclogite-facies rocks during its upwelling and extrusion. A great depth of serpentinization is consistent with the occurrence of antigorite surrounding the tectonic blocks. Recently, Tsujimori et al. (2006a) reevaluated the peak *P-T* condition of Franciscan eclogites of the Tiburon Peninsula as P = 2.2–2.5 GPa and T = 550–620 °C, and they suggested that the Franciscan high-grade blocks were subducted to depths of ~75–80 km (Fig. 8). Although we could not constrain the maximum pressure of the New Idria eclogites, it can be speculated that the New Idria eclogites also experienced such a great depth.

On the other hand, the New Idria garnet-amphibolite that recorded a lower-pressure and higher-temperature condition might have been incorporated into the New Idria serpentinite diapir at a depth near the crust-mantle boundary. Our preliminary K-Ar dating for hornblende separates (0.17 wt% K) from the investigated CGA sample yields 135 ± 7 Ma. This cooling age gives the minimum age of the upwelling of the New Idria serpentinite diapir.

Many Franciscan high-grade blocks have experienced various degrees of blueschist-facies overprinting (e.g., Wakabayashi, 1990, 1999; Krogh et al., 1994; Tsujimori et al., 2006a). Such a *P-T* path suggests that the rocks were "refrigerated" during exhumation inasmuch as no greenschist- or amphibolite-facies recrystallization took place. However, the occurrence of jadeite in retrograde lawsonite-blueschist mineral assemblages has not been described previously. Among the reported New Idria high-grade blocks, the occurrences of retrograde jadeite (up to 94 mol% jd) and lawsonite imply very high-*P*/*T* conditions during blueschist-facies retrogression with infiltration of fluids (e.g., Tsujimori et al., 2005, 2006b). It is noteworthy that the jadeitite occurrence at Clear Creek is the only known locality in the California Coast Ranges. In general, jadeitite is closely associated with serpentinite, and its formation requires high-*P*/*T* conditions (P > 1.0 GPa at T = 200–400 °C) and infiltration of Na- and Al-rich alkaline fluid to the serpentinite (Harlow and Sorensen, 2005). Considering the jadeitite-bearing unusual retrograde mineral assemblage of the investigated blocks, the blueschist-facies recrystallization (M_2) was probably synchronous with the formation of jadeitite in the New Idria serpentinite.

Origin of the New Idria Serpentinite Diapir

The finding of high-grade blocks in the New Idria serpentinite indicates a relatively deep origin of serpentinite. Based on available petrotectonic information of ophiolitic rocks in the California continental margin, and geophysical data for modern subduction zones, the following three possible protoliths of the New Idria serpentinite should be considered:

Model I: Underplated Abyssal Peridotite in Accretionary Complex

Coleman (2000) suggested that the New Idria serpentinite had been part of an abyssal peridotite within a fracture zone exposed on the leading edge of the Farallon plate as it entered the Franciscan subduction trench mélange. Moderately depleted harzburgite relics in the New Idria serpentinite are consistent with abyssal peridotite from fracture zones (e.g., Dick and Bullen, 1984). This model suggests that the partially serpentinized fracture-zone peridotite was detached during subduction and became part of the Franciscan Complex that wedged under the Great Valley Group (Wentworth et al., 1984). The lighter and rheologically weaker serpentinite can move upward and laterally, lubricating the west-directed blind thrust fault (e.g., Coleman, 1980).

Model II: Dismembered Mantle Section of the Coast Range Ophiolite

The basement of the Great Valley Group is the Coast Range ophiolite that formed as part of an intraoceanic arc system in the Late Jurassic (172–165 Ma) (e.g., Coleman, 1986, 2000; Hopson et al., 1981; Godfrey and Klemperer, 1998). The Coast Range ophiolite displays incomplete ophiolitic sequences and in some places is dismembered, forming serpentinite mélanges. The magnetic modeling of the New Idria serpentinite by Jachens et al. (1995) suggested a steeply east-dipping and detached magnetic body (serpentinite mélange) extending into the Franciscan Complex. It is possible that the high-grade tectonic blocks have been tectonically emplaced into the Coast Range serpentinized mantle beneath the Great Valley Group.

Model III: Serpentinized Forearc Mantle Wedge

Recently, numerous geophysical transects were completed across the arc-trench system in Japan, Cascadia along western North America, and Izu-Bonin-Mariana image serpentinized mantle wedge along the hanging-wall boundary of the trench (e.g., Kamiya and Kobayashi, 2000; Kamimura et al., 2002; Bostock et al., 2002; Zhang et al., 2004; Seno, 2005). These geophysical observations are consistent with an idea that low-viscous serpentinite can produce a buoyancy-driven return flow necessary to exhume high-pressure rocks from subduction zones (e.g., Guillot et al., 2000). If we adopt this model, the New Idria serpentinite does not need to correlate with either abyssal peridotite or Coast Range ophiolite. Instead, it may represent part of serpentinized mantle wedge that extruded with blocks of high-pressure rocks.

ACKNOWLEDGMENTS

We dedicate this paper to our close friend and mentor, W. Gary Ernst, who was the first to relate high-*P*/*T* Franciscan metamorphism to subduction. This research was supported financially in part by Japanese Society for the Promotion of Science Research Fellowship for Research Abroad of the first author. Preparation of this manuscript was supported by National Science Foundation grant EAR-0003355. The first author thanks A. Ishiwatari, who accompanied him on a field trip to New Idria in 1994. This manuscript was considerably improved by the comments and suggestions of reviewers John Wakabayashi, Carl Jacobson, Gary Ernst, and Chris Mattinson.

REFERENCES CITED

Anczkiewicz, B., Platt, J.P., Thirlwall, M.F., and Wakabayashi, J., 2004, Franciscan subduction off to a slow start: Evidence from high-precision Lu-Hf garnet ages on high-grade blocks: Earth and Planetary Science Letters, v. 225, p. 147–161, doi: 10.1016/j.epsl.2004.06.003.

Arai, S., 1994, Compositional variation of olivine-chromian spinel in Mg-rich magmas as a guide to their residual spinel peridotites: Journal of Volcanology and Geothermal Research, v. 59, p. 279–293.

Armstrong, J.T., 1988, Quantitative analysis of silicate and oxide minerals: Comparison of Monte Carlo, ZAF and Phi-Rho-Z procedures, *in* Newbury, D.E., ed., Analysis microbeam: San Francisco, California, San Francisco Press, p. 239–246.

Atwater, B.F., Trumm, D.A., Tinsley, J.C.I., Stein, R.S., Tucker, A.B., Donahue, D.J., Jull, A.J.T., and Payen, L.A., 1989, Alluvial plains and earthquake recurrence at the Coalinga anticline, *in* Rymer, M.J., and Ellsworth, W.L., eds., The Coalinga, California, earthquake of May 2, 1983: U.S. Geological Survey Professional Paper 1487, p. 273–297.

Banno, S., Shibakusa, H., Enami, M., Wang, C.-L., and Ernst, W.G., 2000, Chemical fine structure of Franciscan jadeitic pyroxene from Ward Creek, Cazadero area, California: American Mineralogist, v. 85, p. 1795–1798.

Bate, M.A., 1985, Depositional sequence of Temblor and Big Blue Formations, Coalinga anticline, California, *in* Graham, S.A., ed., Geology of the Temblor Formation, western San Joaquin basin, California: Pacific Section, Society of Economic Paleontologists and Mineralogists, v. 44, p. 69–86.

Bostock, M.G., Hyndman, R.D., Rondenay, S., and Peacock, S.M., 2002, An inverted continental Moho and serpentinization of the forearc mantle: Nature, v. 417, p. 536–538, doi: 10.1038/417536a.

Brown, E.H., and Bradshaw, J.Y., 1979, Phase relations of pyroxene and amphibole in greenstone, blueschist, and eclogite of the Franciscan Complex, California: Contributions to Mineralogy and Petrology, v. 71, p. 67–83, doi: 10.1007/BF00371882.

Casey, T.A.L., and Dickinson, W.R., 1976, Sedimentary serpentinite of the Miocene Big Blue Formation near Cantua Creek, California, *in* Fritsche, A.E., et al., eds., The Neogene Symposium: Selected technical papers on paleontology, sedimentology, petrology, tectonics and geologic history of the Pacific coast of North America: San Francisco, California, Society of Economic Paleontologists and Mineralogists, p. 65–74.

Cloos, M., 1986, Blueschists in the Franciscan Complex of California: Petrotectonic constrains on uplift mechanism: Geological Society of America Memoir 164, p. 77–93.

Coleman, R.G., 1961, Jadeite deposits of the Clear Creek area, New Idria district, San Benito County, California: Journal of Petrology, v. 2, p. 209–247.

Coleman, R.G., 1980, Tectonic inclusions in serpentinites: Archives des Sciences, Société de Physique et d'Histoire Naturelle de Genève, v. 33, p. 89–102.

Coleman, R.G., 1986, Ophiolites and accretion of the North American Cordillera: Bulletin de la Société Géologique de France, v. II, no. 8, p. 961–968.

Coleman, R.G., 1996, New Idria serpentinite: A land management dilemma: Environmental and Engineering Geosciences, v. 2, p. 9–22.

Coleman, R.G., 2000, Prospecting for ophiolites along the California continental margin, *in* Dilek, Y., et al., eds., Ophiolites and oceanic crust: New insights from field studies and the Ocean Drilling Program: Geological Society of America Special Paper 349, p. 351–364.

Coleman, R.G., and Lanphere, M.A., 1971, Distribution and age of high-grade blueschists, associated eclogites, and amphibolites from Oregon and California: Geological Society of America Bulletin, v. 82, p. 2397–2412.

Cowan, D.S., 1979, Serpentinite flows on Joaquin Ridge, southern Coast Ranges, California: Geological Society of America Bulletin, v. 81, p. 2615–2628.

Dibblee, T.W.Jr., 1972, Preliminary geologic map of the San Jose East quadrangle: Santa Clara County, California: U.S. Geological Survey Open-File Report, v. 72-92, scale 1:24,000.

Dick, H.J.B., and Bullen, T., 1984, Chromian spinel as a petrogenetic indicator in abyssal and Alpine-type peridotites and spatially associated lavas: Contributions to Mineralogy and Petrology, v. 86, p. 54–76, doi: 10.1007/BF00373711.

Dickinson, W.R., 2002, Reappraisal of hypothetical Franciscan thrust wedging at Coalinga: Implications for tectonic relations along the Great Valley flank of the California Coast Ranges: Tectonics, v. 21, doi: 10.1029/2001TC001315.

Eckel, E.B., and Myers, W.B., 1946, Quicksilver deposits of the New Idria district, San Benito and Fresno Counties, California: California Division of Mines and Geology Bulletin, v. 42, p. 81–124.

Ernst, W.G., 1971, Petrologic reconnaissance of Franciscan metagraywackes from the Diablo Range, central California Coast Ranges: Journal of Petrology, v. 12, p. 413–437.

Ernst, W.G., and Liu, J., 1998, Experimental phase-equilibrium study of Al- and Ti-contents of calcic amphibole in MORB—A semiquantitative thermobarometer: American Mineralogist, v. 83, p. 952–969.

Fryer, P., Mottl, M., Johnson, L., Haggerty, J., Phipps, S., and Maekawa, H., 1995, Serpentine bodies in the forearcs of Western Pacific convergent margins: Origin and associated fluids: American Geophysical Union Geophysical Monograph 88, p. 259–280.

Godfrey, N.J., and Klemperer, S.L., 1998, Ophiolitic basement to a forearc basin and implications for continental growth: The Coast Range / Great Valley ophiolite, California: Tectonics, v. 17, p. 558–570, doi: 10.1029/98TC01536.

Guillot, S., Hattori, K., and de Sigoyer, J., 2000, Mantle wedge serpentinization and exhumation of eclogites: Insights from eastern Ladakh, northwest Himalaya: Geology, v. 28, p. 199–202, doi: 10.1130/0091-7613(2000)028<0199:MWSAEO>2.3.CO;2.

Harlow, G.E., 1999, Interpretation of Kcpx and CaEs components in clinopyroxene from diamond inclusions and mantle samples, *in* Gurney, J.J., et al., eds., Proceedings of Seventh International Kimberlite Convention: Cape Town, Redroof Design, v. 1, p. 321–331.

Harlow, G.E., and Sorensen, S.S., 2005, Jade (nephrite and jadeitite) and serpentinite: Metasomatic connections: International Geology Review, v. 47, p. 113–146.

Holland, T.J.B., 1983, The experimental determination of activities in disordered and short-range ordered jadeitic pyroxenes: Contributions to Mineralogy and Petrology, v. 82, p. 214–220, doi: 10.1007/BF01166616.

Hopson, C.A., Mattinson, J.M., and Pessagno, E.A., Jr., 1981, Coast Range ophiolite, western California, *in* Ernst, W.G., ed., The geotectonic development of California (Rubey Volume I): Englewood Cliffs, New Jersey, Prentice-Hall, p. 418–510.

Huot, F., and Maury, R.C., 2002, The Round Mountain serpentinite mélange, northern Coast Ranges of California: An association of backarc and arc-related tectonic units: Geological Society of America Bulletin, v. 114, p. 109–123, doi: 10.1130/0016-7606(2002)114<0109:TRMSML>2.0.CO;2.

Ishii, T., Robinson, P.T., Maekawa, H., and Fiske, R., 1992, Petrological studies of peridotites from diapiric serpentinite seamounts in the Izu-Ogasawara-Mariana forearc, Leg 125, *in* Fryer, P., Pearce, J.A., Stokking, L.B., and the Leg 125 Scientific Shipboard Party, eds., Proceedings of the Ocean Drilling Program, Scientific Results, Volume 125: College Station, Texas, Ocean Drilling Program, p. 445–485.

Jachens, R.C., Griscom, A., and Roberts, C.W., 1995, Regional extent of Great Valley basement west of the Great Valley, California: Implications for extensive tectonic wedging in the California Coast Ranges: Journal of Geophysical Research, v. 100, p. 12,769–12,790, doi: 10.1029/95JB00718.

Johnson, C.M., and O'Neil, J.R., 1984, Triple junction magmatism: A geochemical study of Neogene volcanic rocks in western California: Earth and Planetary Science Letters, v. 71, p. 241–263, doi: 10.1016/0012-821X(84)90090-6.

Kamimura, A., Kasahara, J., Shinohara, M., Hino, R., Shiobara, H., Fujie, G., and Kanazawa, T., 2002, Crustal structure study at the Izu-Bonin subduction zone around 31°N: Implications of serpentinized materials along the subduction plate boundary: Physics of the Earth and Planetary Interiors, v. 132, p. 105–129, doi: 10.1016/S0031-9201(02)00047-X.

Kamiya, S., and Kobayashi, Y., 2000, Seismological evidence for the existence of serpentinized wedge mantle: Geophysical Research Letters, v. 27, p. 819–822, doi: 10.1029/1999GL011080.

Kretz, R., 1983, Symbols for rock-forming minerals: American Mineralogist, v. 68, p. 277–279.

Krogh, E.J., Oh, C.W., and Liou, J.G., 1994, Polyphase and anticlockwise *P-T* evolution for Franciscan eclogites and blueschists from Jenner, California, USA: Journal of Metamorphic Geology, v. 12, p. 121–134.

Krogh-Ravna, E., 2000, The garnet–clinopyroxene Fe^{2+}–Mg geothermometer: An updated calibration: Journal of Metamorphic Geology, v. 18, p. 211–219, doi: 10.1046/j.1525-1314.2000.00247.x.

Laurs, B.M., Rohtert, W.R., and Gary, M., 1997, Benitoite from the New Idria district, San Benito County, California: Gems and Gemology, v. 33, p. 166–187.

Leake, B.E., Woolley, A.R., Arps, C.E.S., Birch, W.D., Gilbert, M.C., Grice, J.D., Hawthorne, F.C., Kato, A., Kisch, H.J., Krivovichev, V.G., Linthout, K., Laird, J., Mandarino, J.A., Maresch, W.V., Nickel, E.H., Rock, N.M.S., Schumacher, J.C., Smith, D.C., Stephenson, N.C.N., Ungaretti, L., Whittaker, E.J.W., and Guo, Y.Z., 1997, Nomenclature of amphiboles: Report of the subcommittee on amphiboles of the International Mineralogical Association, commission on new minerals and mineral names: American Mineralogist, v. 82, p. 9–10.

Liou, J.G., Tsujimori, T., Zhang, R.Y., Katayama, I., and Maruyama, S., 2004, Global UHP metamorphism and continental subduction/collision: The Himalayan model: International Geology Review, v. 46, p. 1–27.

Liu, J., Bohlen, S.R., and Ernst, W.G., 1996, Stability of hydrous phases in subducting oceanic crust: Earth and Planetary Science Letters, v. 143, p. 161–171, doi: 10.1016/0012-821X(96)00130-6.

Loney, R.A., Himmelberg, G.R., and Coleman, R.G., 1971, Structure and petrology of the Alpine-type peridotite at Burro Mountain, California, U.S.A.: Journal of Petrology, v. 12, p. 245–309.

Maekawa, H., Shozui, M., Ishii, T., Fryer, P., and Pearce, J.A., 1993, Blueschist metamorphism in an active subduction zone: Nature, v. 364, p. 520–523, doi: 10.1038/364520a0.

Maruyama, S., and Liou, J.G., 1987, Clinopyroxenes—A mineral telescoped through the processes of blueschist facies metamorphism: Journal of Metamorphic Geology, v. 5, p. 529–552.

Maruyama, S., and Liou, J.G., 1988, Petrology of Franciscan metabasites along the jadeite-glaucophane type facies series, Cazadero, California: Journal of Petrology, v. 29, p. 1–37.

Morimoto, N. Fabries, J., Ferguson, A.K., Ginzburg, I.V., Ross, M., Seifert, F.A., Zussman, J., Aoki, K., and Gottardi, G., 1988, Nomenclature of pyroxenes: American Mineralogist, v. 73, p. 1123–1133.

Miura, R., Nakamura, Y., Tokuyama, H., and Coffin, M.F., 2004, "Rootless" serpentinite seamount on the southern Izu-Bonin forearc: Implications for basal erosion at convergent plate margins: Geology, v. 32, p. 541–544, doi: 10.1130/G20319.1.

Moore, D.E., and Black, M.C., Jr., 1989, New evidence for polyphase metamorphism of glaucophane schist and eclogite exotic blocks in the Franciscan Complex, California and Oregon: Journal of Metamorphic Geology, v. 7, p. 211–228.

Namson, J., Davis, T.L., and Lagoe, M.B., 1989, Tectonic history and thrust-fold deformation style of seismically active structures near Coalinga, California, *in* Rymer, M.J., and Ellsworth, W.L., eds., The Coalinga, California, earthquake of May 2, 1983: U.S. Geological Survey Professional Paper 1487, p. 79–96.

Nilsen, T.H., 1984, Offset along the San Andreas fault of Eocene strata from the San Juan Bautista area and western San Emigdio Mountains, California: Geological Society of America Bulletin, v. 95, p. 599–609, doi: 10.1130/0016-7606(1984)95<599:OATSAF>2.0.CO;2.

Obradovich, J.D., Kunk, M.J., and Lanphere, M.A., 2000, Age and paragenesis of the unique mineral benitoite: Geological Society of America Abstracts with Programs, v. 32, no. 7, p. 440.

Oh, C.W., and Liou, J.G., 1990, Metamorphic evolution of two different eclogites in the Franciscan Complex, California, USA: Lithos, v. 25, p. 41–53, doi: 10.1016/0024-4937(90)90005-L.

Peacock, S.M., and Wang, K., 1999, Seismic consequences of warm versus cool subduction metamorphism: Examples from southwest and northeast Japan: Nature, v. 286, p. 937–939.

Saha, A., Basu, A.R., Wakabayashi, J., and Wortman, G.L., 2005, Geochemical evidence for a subducted infant arc in Franciscan high-grade-metamorphic tectonics blocks: Geological Society of America Bulletin, v. 117, p. 1318–1335, doi: 10.1130/B25593.1.

Seno, T., 2005, Variation of downdip limit of the seismogenic zone near the Japanese islands: Implications for the serpentinization mechanism of the forearc mantle wedge: Earth and Planetary Science Letters, v. 231, p. 249–262, doi: 10.1016/j.epsl.2004.12.027.

Sorensen, S.S., 1988, Petrology of amphibolite-facies mafic and ultramafic rocks from the Catalina Schist, southern California: Metamorphism and migmatization in a subduction zone metamorphic setting: Journal of Metamorphic Geology, v. 6, p. 405–435.

Tsujimori, T., 1997, Omphacite-diopside vein in an omphacitite block from the Osayama serpentinite mélange, Sangun-Renge metamorphic belt, southwestern Japan: Mineralogical Magazine, v. 61, p. 845–852.

Tsujimori, T., and Liou, J.G., 2004, Coexisting chromian omphacite and diopside in tremolite schist from the Chugoku Mountains, SW Japan: The effect of Cr on the omphacite-diopside immiscibility gap: American Mineralogist, v. 89, p. 7–14.

Tsujimori, T., Liou, J.G., and Coleman, R.G., 2005, Coexisting retrograde jadeite and omphacite in a jadeite-bearing lawsonite eclogite from the Motagua fault zone, Guatemala: American Mineralogist, v. 90, p. 836–842.

Tsujimori, T., Matsumoto, K., Wakabayashi, J., and Liou, J.G., 2006a, Franciscan eclogite revisited: Reevaluation of the *P-T* evolution of tectonic blocks from Tiburon Peninsula, California, USA: Mineralogy and Petrology, v. 88, p. 243–267, doi: 10.1007/s00710-006-0157-1.

Tsujimori, T., Sisson, V.B., Liou, J.G., Harlow, G.E., and Sorensen, S.S., 2006b, Petrologic characterization of Guatemalan lawsonite-eclogite: Eclogitization of subducted oceanic crust in a cold subduction zone, *in* Hacker, B.H., et al., eds., Ultrahigh-pressure metamorphism: Deep continental subduction: Geological Society of America Special Paper 403, p. 147–168.

Ueda, H., Usuki, T., and Kuramoto, Y., 2004, Intraoceanic unroofing of eclogite facies rocks in the Omachi seamount, Izu-Bonin frontal arc: Geology, v. 32, p. 849–852, doi: 10.1130/G20837.1.

Van Baalen, M.R., 2004, Migration of the Mendocino Triple Junction and the origin of titanium-rich mineral suites at New Idria, California: International Geology Review, v. 46, p. 671–692.

Vermeesch, P., Miller, D.D., Graham, S.A., De Grave, J., and McWilliams, M.O., 2006, Multi-method detrital thermochronology of the Great Valley Group near New Idria (California): Geological Society of America Bulletin, v. 118, p. 210–218, doi: 10.1130/B25797.1.

Wakabayashi, J., 1990, Counterclockwise *P-T-t* paths from amphibolites, Franciscan Complex, California: Metamorphism during the early stages of subduction: Journal of Geology, v. 98, p. 657–680.

Wakabayashi, J., 1999, Subduction and the rock record: Concepts developed in the Franciscan Complex, California: Geological Society of America Special Paper 338, p. 123–133.

Wentworth, C.M., Blake, M.C.J., Jones, D.L., and Walter, A.W., 1984, Tectonic wedging associated with emplacement of the Franciscan assemblage, California Coast Ranges, *in* Blake, M.C.J., ed., Franciscan geology of northern California: Los Angeles, California, Pacific Section, Society of Economic Paleontologists and Mineralogists, v. 43, p. 163–173.

Zhang, H., Thurber, C.H., Shelly, D., Ide, S., Beroza, G.C., and Hasegawa, A., 2004, High-resolution subducting slab structure beneath northern Honshu, Japan, revealed by double-difference tomography: Geology, v. 32, p. 361–364, doi: 10.1130/G20261.2.

Manuscript Accepted by the Society 13 July 2006